ORIGINAL ARTICLE

CLINICAL CYTOMETRY WILEY

Multi-site reproducibility of a human immunophenotyping assay in whole blood and peripheral blood mononuclear cells preparations using CyTOF technology coupled with Maxpar Pathsetter, an automated data analysis system

Charles Bruce Bagwell[1] | Benjamin Hunsberger[1] | Beth Hill[1] | Donald Herbert[1] | Christopher Bray[1] | Thirumahal Selvanantham[2] | Stephen Li[2] | Jose C. Villasboas[3] | Kevin Pavelko[3] | Michael Strausbauch[3] | Adeeb Rahman[4] | Gregory Kelly[4] | Shahab Asgharzadeh[5] | Azucena Gomez-Cabrero[5] | Gregory Behbehani[6] | Hsiaochi Chang[6] | Justin Lyberger[6] | Ruth Montgomery[7] | Yujiao Zhao[7] | Margaret Inokuma[1] | Ofir Goldberger[8] | Greg Stelzer[8]

[1]Verity Software House, Topsham, Maine

[2]Fluidigm Canada Inc., Markham, Ontario, Canada

[3]Mayo Clinic Health System, Cannon Falls, Minnesota

[4]Icahn School of Medicine at Mount Sinai, New York, New York

[5]Children's Hospital Los Angeles, Los Angeles, California

[6]Ohio State University, Columbus, Ohio

[7]Yale School of Medicine, New Haven, Connecticut

[8]Fluidigm Corporation, San Francisco, California

Correspondence
C. Bruce Bagwell, PO Box 247, Topsham, ME 04086.
Email: cbb@vsh.com

Abstract

High-dimensional mass cytometry data potentially enable a comprehensive characterization of immune cells. In order to positively affect clinical trials and translational clinical research, this advanced technology needs to demonstrate a high reproducibility of results across multiple sites for both peripheral blood mononuclear cells (PBMC) and whole blood preparations. A dry 30-marker broad immunophenotyping panel and customized automated analysis software were recently engineered and are commercially available as the Fluidigm® Maxpar® Direct™ Immune Profiling Assay™. In this study, seven sites received whole blood and six sites received PBMC samples from single donors over a 2-week interval. Each site labeled replicate samples and acquired data on Helios™ instruments using an assay-specific acquisition template. All acquired sample files were then automatically analyzed by Maxpar Pathsetter™ software. A cleanup step eliminated debris, dead cells, aggregates, and normalization beads. The second step automatically enumerated 37 immune cell populations and performed label intensity assessments on all 30 markers. The inter-site reproducibility of the 37 quantified cell populations had consistent population frequencies, with an average %CV of 14.4% for whole blood and 17.7% for PBMC. The dry reagent coupled with automated data analysis is not only convenient but also provides a high degree of reproducibility within and among multiple test sites resulting in a comprehensive yet practical solution for deep immune phenotyping.

KEYWORDS
cytometry automation, cytometry standardization, kits, percentage precision

1 | INTRODUCTION

Multi-site studies have been successfully performed in flow cytometry, but only a few multi-site mass cytometry studies have been reported (Blazkova et al., 2017; Leipold et al., 2018) and no mass cytometry-based study has examined the reproducibility of whole blood preparations or dry antibody panels. In mass cytometry, the use of an inductively coupled plasma mass spectrometer to detect heavy metal-tagged probes on a single-cell basis mitigates the issue of spectral overlap between detection channels, easily allowing for the use of >40 simultaneous measurements.

Peripheral blood mononuclear cell (PBMC) preparations have useful storage characteristics, which is helpful for doing multi-site studies. However, immunophenotyping of whole blood specimens is an industry-standard for clinical trials and other types of clinical studies. The ability to standardize both PBMC and whole blood immunophenotyping worldwide would have far-reaching ramifications. In a typical flow cytometry experiment workflow, several areas of variability have been identified. Controlling such factors as reagents, sample handling, instrument setup, and data analysis can lead to standardization (Maecker, McCoy, & Nussenblatt, 2012).

This study is part of an initiative to produce a commercially available product that addresses many of the factors important in developing a standardized immune monitoring assay for mass cytometry. The system consists of a dry antibody product capable of identifying many important immune populations, an instrument setup template, and automated cleanup and analysis software that enumerates a broad spectrum of immune cell types. The core of the panel is based on the recommendation of the Human ImmunoPhenotyping Consortium of the Human Immunology Project (Finak et al., 2016; Maecker et al., 2012). Eight additional antibodies (CD28, CD45, CD57, CD66b, CD294, CD161, CXCR5, and TCRγδ) were added to the panel to better delineate T-cells, NK cells, and granulocytes, and one marker was dropped (CD24). In addition to the antibodies, the dry antibody cocktail also includes rhodium for the discrimination of live/dead cells (Ornatsky et al., 2008). The details of the 30-marker panel are shown in Table 1, and the workflow is shown in Figure 1.

The analysis of the panel was performed by Maxpar Pathsetter software, which uses probability state modeling (PSM) (Bagwell, 2010; Bagwell et al., 2015; Bagwell et al., 2018, Leipold, Maecker, & Stelzer, 2016) to obtain frequencies for 37 immune populations (see Table 2 for model phenotype definitions) as well as stain assessments for all 30 markers. PSM-derived results have been previously shown to correlate well with manual gating (Herbert, Miller, & Bagwell, 2012; Li et al., 2018, 2019; Miller, Hunsberger, & Bagwell, 2012; Wong et al., 2014; Wong, Hunsberger, Bruce Bagwell, & Davis, 2013). Many different validation tests needed to be performed prior to releasing this product. These tests included liquid versus dry panel, intra-assay repeatability, intermediate precision, manual gating versus modeling correlations, and inter-site reproducibility. Most of these validations are presented in a publicly available white paper. Deep Immune Profiling with the Maxpar Direct Immune Profiling System 400247 A2) and data from other tests have been added

TABLE 1 Maxpar direct immune profiling assay 30-marker panel with clones and heavy metals

Target	Clone	Metal
Anti-human CD45	HI30	89Y
Live/dead 103Rh-Intercalator (500 μM)	N/A	103Rh
Anti-human CD196/CCR6	G034E3	141Pr
Anti-human CD123	6H6	143Nd
Anti-human CD19	HIB19	144Nd
Anti-human CD4	RPA-T4	145Nd
Anti-human CD8a	RPA-T8	146Nd
Anti-human CD11c	Bu15	147Sm
Anti-human CD16	3G8	148Nd
Anti-human CD45RO	UCHL1	149Sm
Anti-human CD45RA	HI100	150Nd
Anti-human CD161	HP-3G10	151Eu
Anti-human CD194/CCR4	L291H4	152Sm
Anti-human CD25	BC96	153Eu
Anti-human CD27	O323	154Sm
Anti-human CD57	HCD57	155Gd
Anti-human CD183/CXCR3	G025H7	156Gd
Anti-human CD185/CXCR5	J252D4	158Gd
Anti-human CD28	CD28.2	160Gd
Anti-human CD38	HB-7	161Dy
Anti-human CD56/NCAM	NCAM16.2	163Dy
Anti-human TCRgd	B1	164Dy
Anti-human CD294	BM16	166Er
Anti-human CD197/CCR7	G043H7	167Er
Anti-human CD14	63D3	168Er
Anti-human CD3	UCHT1	170Er
Anti-human CD20	2H7	171Yb
Anti-human CD66b	G10F5	172Yb
Anti-human HLA-DR	LN3	173Yb
Anti-human IgD	IA6-2	174Yb
Anti-human CD127	A019D5	176Yb

to the Supporting Information. The purpose of this study is to report in detail on the last stage of validation where the reproducibility of the kit/analysis system was evaluated by multiple sites for both PBMC and whole blood samples from healthy human subjects.

2 | MATERIALS AND METHODS

2.1 | Study sites

A total of seven sites (six in the United States plus Fluidigm Canada) were selected to participate in these reproducibility studies. These sites are designated as Sites 1, 2, 3, 4, 5, 6, and 7. Site 1 received whole blood products in Week 1 of the study, for which it is designated as Site 1A, and in the second week of the study received whole
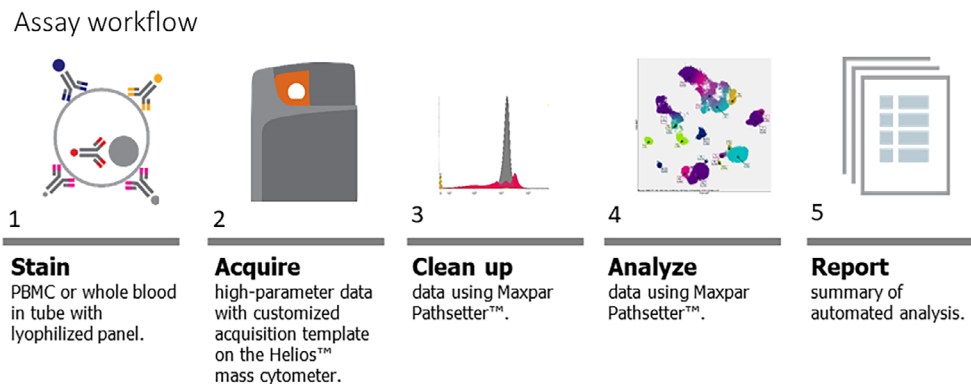
Assay workflow

FIGURE 1 Assay workflow. Based on the broad immune cell phenotyping flow panels for the Human Immune Project (Maecker et al., 2012), the Maxpar Direct Immune Profiling Assay was designed as an optimized panel of 30 dry antibodies plus DNA intercalators in a single tube for staining whole blood and PBMC. Data were acquired on a Fluidigm Helios and analyzed using Maxpar Pathsetter, a customized automated analysis system powered by GemStone 2.0. Pathsetter software automatically cleans the data file by eliminating dead cells, debris, aggregates, and normalization beads. Modeling software then identifies and enumerates a broad spectrum of immune populations and presents the results in summary reports [Color figure can be viewed at wileyonlinelibrary.com]

blood products from a second draw from the same donor, for which it is designated as Site 1B. Site 1 did not participate in the PBMC part of the study. Sites 2, 3, and 4 received whole blood and PBMC samples in Week 1, and Sites 5, 6, and 7 received the products in the second week. All sites were given careful instructions on the staining and analysis procedures, and Fluidigm Field Application Specialists were on hand to provide general guidance on all the procedures.

2.2 | Whole blood collection and shipping

Human whole blood was obtained from Discovery Life Sciences (Huntsville, AL). Whole blood from a single healthy donor was collected into eight individual BD Vacutainer® blood collection tubes containing heparin as an anticoagulant. Two tubes of the whole blood were shipped on cold packs to each study site overnight in a temperature-controlled shipping container.

2.3 | Whole blood staining

An additional heparin blocking step was performed (100 U/ml) for 20 min at room temperature to reduce nonspecific binding between metal-tagged antibodies and eosinophils (Rahman, Tordesillas, & Berin, 2016). Afterward, 270 μl of blood was added directly to four dry antibody tubes and allowed to incubate for 30 min at room temperature. Immediately following staining, erythrocytes were lysed by the addition of 250 μl of Cal-Lyse directly to the staining tube. The tubes were gently vortexed and allowed to incubate for 10 min at room temperature followed by the addition of 3 ml of Maxpar water and an additional 10 min of incubation. The tubes were washed three times in Maxpar Cell Staining Buffer (CSB) followed by fixation in 1.6% paraformaldehyde for 10 min. Following fixation, the cells were spun to a pellet, the fixative removed, and the pellet was resuspended in 1 ml of the 125 nm Cell-ID™ Intercalator-Ir (Ornatsky et al., 2008) and incubated overnight at 4° (See Figure 1 for the assay workflow).

2.4 | PBMC specimens

One lot of cryopreserved PBMC from a single healthy donor was obtained from a commercial biological specimen supply source (Discovery Life Sciences) and reserved as the reference lot for the study. Two vials of cryopreserved PBMC were shipped on dry ice to each of six sites. The PBMC samples were thawed based on the manufacturer's (Discovery Life Sciences) recommendations, which was to thaw in serum-free media with no anti-aggregate.

2.5 | PBMC staining

A vial of cryopreserved PBMC was thawed and washed. The viability and cell count were determined and the cells were washed in CSB. After the wash, the cells were resuspended in CSB to a concentration of 6×10^7 cells/ml. FC receptors were blocked by adding 5 μl of Human TruStain FcX to 3×10^6 cells in 50 μl and incubated for 10 min. About 215 μl of CSB was then added to the PBMC. About 270 μl of the PBMC was added directly added to each of the four dry antibody tubes for antibody staining (see Table 1). After a 30-min incubation, the cells were washed twice in CSB, followed by fixation in 1.6% paraformaldehyde for 10 min. Following fixation, the cells were spun to a pellet, the fixative was removed, and the pellet was resuspended in 1 ml of the 125 nM Cell-ID Intercalator-Ir and incubated overnight at 4°.

2.6 | Sample acquisition

Following the overnight incubation, the PBMC fixed cells were washed twice in CSB and twice with Maxpar Cell Acquisition Solution (CAS) with a final resuspension of the cells at 1×10^6 cells/ml in CAS containing 0.1× EQ™ Four Element Calibration Beads. Whole blood sample acquisition was also performed the next day post staining on a Helios system utilizing CyTOF® Software version 6.7.1016 using the Maxpar Direct Immune Profiling Assay template. All instruments were

TABLE 2 Immune cell populations and model definitions

Index	Populations	Model phenotypes
1	Lymphocytes	CD3 T cells + B cells + NK cells + plasmablasts
2	CD3 T cells	CD8 T cells + CD4 T cells + γδ T cells + MAIT/NKT cells
3	CD8 T cells	CD3+ CD66b- CD19- CD8+ CD4- CD14- CD161- TCRgd- CD123- CD11c-
4	CD8 naïve	CD8 T cells + CD45RA+ CCR7+ CD27+
5	CD8 central memory	CD8 T cells + CD45RA- CCR7+ CD27+
6	CD8 effector memory	CD8 T cells + CCR7- CD27+
7	CD8 terminal effector	CD8 T cells + CCR7- CD27-
8	CD4 T cells	CD66b- CD3+ CD8- CD4+ CD14- TCRgd- CD11c-
9	CD4 naïve	CD4 T cells + CD45RA+ CCR7+ CD27+
10	CD4 central memory	CD4 T cells + CD45RA- CCR7+ CD27+
11	CD4 effector memory	CD4 T cells + CD45RA- CCR7- CD27+
12	CD4 terminal effector	CD4 T cells + CD45RA- CCR7- CD27-
13	Tregs	CD4 T cells + CD25+ CD127- CCR4+
14	Th1-like	CD4 T cells + CXCR3+ CCR6- CXCR5- CCR4-
15	Th2-like	CD4 T cells + CXCR3- CCR6- CXCR5- CCR4+
16	Th17-like	CD4 T cells + CXCR3- CCR6+ CXCR5- CCR4+
17	γ T cells	CD66b- CD3+ CD8dim,- CD4- CD14- TCRgd dim,+
18	MAIT/NKT cells	CD66b- CD3+ CD4- CD14- CD161+ TCRgd- CD28+ CD16-
19	B cells	CD3- CD14- CD56- CD16 dim,- CD19+ CD20+ HLA-DR dim,+
20	B naïve	B cells + CD27-
21	B memory	B cells + CD27+
22	Plasmablasts	CD3- CD14- CD16-,dim CD66b- CD20- CD19+ CD56- CD38++ CD27+
23	NK cells	CD14- CD3- CD123- CD66b- CD45RA+ CD56 dim,+
24	NK early	NK cells + CD57-
25	NK late	NK cells + CD57+
26	Monocytes	CD3- CD19- CD56- CD66b- HLA-DR+ CD11c+
27	Monocytes classical	Monocytes + CD14+ CD38+
28	Monocytes transitional	Monocytes + CD14 dim CD38 dim
29	Monocytes non-classical	Monocytes + CD14- CD38-
30	DCs	pDCs + mDCs
31	pDCs	CD3- CD19- CD14- CD20- CD66b- HLA-DR dim,+ CD11c- CD123+
32	mDCs	CD3- CD19- CD14- CD20- HLA-DR dim,+ CD11c dim,+ CD123- CD16 dim,- CD38 dim,+ CD294- HLA-D
33	Granulocytes	Neutrophils + basophils + eosinophils + CD66b- neutrophils
34	Neutrophils	CD66b dim,+ CD16+ HLA-DR-
35	Basophils	HLA-DR- CD66b- CD123 dim,+ CD38+ CD294+
36	Eosinophils	CD14- CD3- CD19- HLA-DR- CD294+ CD66b dim,+
37	CD66b- neutrophils	CD3- CD19- CD66b- CD56- HLA-DR- CD123- CD45-

The above table shows the 37 immune cell populations enumerated and their associated model phenotypes.
The modeling algorithm is designed to fit the measurements in the order listed by the phenotype. Nomenclature such as TCRγδ dim,+ means that dim to positive events were selected. Occasionally the same marker is modeled twice, where the first time is a broader classification and the last time is a more specific classification. See Section 4 for details on the subsetting and staging rationales for monocytes, CD8 T-cells, and CD4 T-cells.

equipped with a WB Injector, and all samples were acquired in CAS containing 0.1× EQ beads. Prior to the start of the study, all instruments were evaluated to ensure performance at above the minimum Helios system specifications for calibration. Following the instrument tuning and bead sensitivity test, the system was preconditioned with CAS. A minimum of 400,000 events for whole blood and 300,000 events for PBMC were acquired per file at a typical acquisition rate of 250–500 events/s.

FIGURE 2 Cleanup and analysis Cen-se' maps: The top two panels are Cen-se' maps created from the QC measurements: DNA1, DNA2, Live/ Dead, Beads, Event Length, Residual, Center, Width, and Offset. The top-left panel represents the raw normalized data from one file and the top-right the associated cleaned exported data. In the top-left panel, A (dark gray) are the live intact events, B (blue) are the low-DNA1 or debris events, C (yellow) are the normalization beads, D (blue) are events with zero pulse-processing parameters (Residual, Center, Width, and Offset), E (red) are "not cleaned events" with high Residual and Event Lengths, F (red) are true aggregates with high DNA1 and DNA2 intensities, G (yellow) are bead/cell aggregates, and H (red) are coincident ion clouds with low and high center values. The top-right panel is the Cen-se' map of only the "cleaned" events. The bottom panel shows the same data with all markers selected after cleanup and modeling [Color figure can be viewed at wileyonlinelibrary.com]

A: Intact live cells
B: Debris
C: Normalization beads
D: Aborted pulse processing
E: High event length and residual
F: True aggregates (doublets/triplets)
G: Bead/cell aggregate
H: Coincident ion clouds
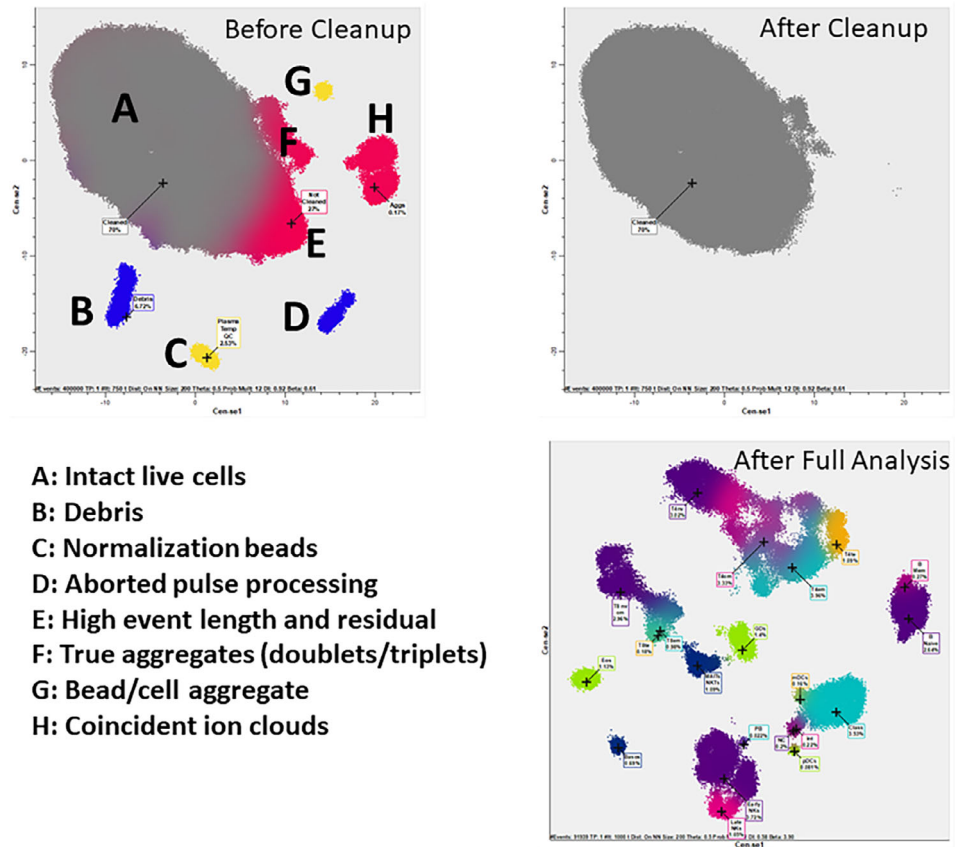
2.7 | Data normalization

After acquisition, data were normalized using the CyTOF Software v. 6.7.1016. This method normalizes the data to a global standard, called a bead passport, determined for each log of EQ beads. This passport contains a profile of mean Di counts of all the masses for a particular lot of the beads as determined by multiple measurements during the manufacture of the EQ beads. The normalization factor is the ratio of passport median Di values to bead singlet population median Di values of the encoding isotopes. Isotopes in the EQ beads cover the mass range measurable on the CyTOF instrument. The normalization factors for mass channels between the encoding isotopes are linearly interpolated. All mass channel values for all events are then multiplied by these normalization factors to obtain the normalized values, and data are written to the normalized file.

2.8 | Data analysis

FCS files generated by the Helios were analyzed by Maxpar Pathsetter, an automated analysis system powered by GemStone™ 2.0.41 (Verity Software House, Topsham, ME). Initial analyses process raw normalized FCS3.0 files with a specially designed Cleanup PSM model. The Cleanup model leverages Gaussian pulse-processing parameters such as Center, Width, Offset, and Residual as well as DNA intercalators to eliminate unwanted events. Subsequent to cleanup, the program produces new FCS3.0 files consisting of only intact live singlet cells. This new cleaned file is then processed by an

automated analysis of a second model, which also uses PSM to identify and label the major immune cell populations in sample files.

This system is integrated with dimensionality-reduction mapping known as Cauchy Enhanced Nearest-neighbor Stochastic Embedding (Cen-se'™), which generates a visual display of high-dimensional data labeled with the major cell populations. Figure 2 shows a Cen-se' map of only QC measurements from one of the whole blood files in the study before and after the cleanup procedure (see top-left and right panels) as well as a map of all markers after full analysis (see bottom-right panel). All analyses were done on the same mid-level PC (Intel® Core™ i7-6700 CP @3.40 GHz RAM: 24 GB x64-based processor). The average run time for the whole blood Cleanup Stage was 37.3 s with a range of 36.5–37.9. The run time statistics for the other parts of the study were PBMC Cleanup Stage: 33.2 s (32.2–39.7), whole blood Phenotyping and Cen-se' Stage: 207.7 s (137.3–227.9), PBMC Phenotyping and Cen-se' Stage: 233.6 s (212.8–282.1). The complete average analysis time for the whole blood samples was 4.1 min and for PBMCs, 4.4 min.

3 | RESULTS

3.1 | Whole blood

A total of 32 whole blood-derived files from seven different sites were analyzed by the cleanup phase of the analysis (see Table 3 for a summary of the results). On average, 70.9% of the events were considered desirable "live intact cells"; 26.9% were excluded because they were classified as dead cells, debris, true aggregates, aborted pulses,

TABLE 3 Whole blood cleanup summary statistics

Multi-site whole blood reproducibility study: Cleanup statistics[a]

Site	Replicate	%Clean[b]	%Excluded	%Beads	%Unclass[c]	%Debris	%Dead	%Aggs	CeO$_2$ ratio	Acq rate	%CD19+ CD3+[d]	%CD14+ CD3+[e]	Total cells	Run time[f]
Site 1A	1	65.1	32.7	1.9	0.4	9.9	0.1	13.8	1.6	406.1	0.3	0.5	400,000	37.1
	2	61.4	36.1	1.6	1.0	14.6	0.2	12.3	1.7	410.7	0.3	1.0	400,000	37.7
	3	65.8	32.4	1.4	0.5	11.9	0.1	11.7	1.3	353.0	0.2	0.4	400,000	37.9
	4*	51.9	45.0	1.2	1.8	27.3	0.8	9.3	1.5	444.9	0.2	21.5	400,000	37.5
Site 2	1	72.4	24.9	2.5	0.2	7.4	0.1	8.4	1.8	244.1	0.2	0.5	400,000	37.5
	2	72.5	24.8	2.5	0.2	6.4	0.1	9.1	1.8	269.4	0.2	0.5	398,479	37.2
	3	71.0	26.8	2.1	0.2	9.5	0.1	8.2	1.8	272.9	0.2	0.5	400,000	37.7
	4	75.0	22.5	2.4	0.1	4.9	0.1	9.0	1.8	246.3	0.2	0.6	400,000	37.0
Site 3	1	69.2	26.9	3.6	0.3	12.8	0.0	7.5	0.8	264.7	0.2	0.3	400,000	37.2
	2	61.4	34.8	3.3	0.5	20.6	0.0	7.7	1.9	260.4	0.2	0.5	400,000	37.2
	3	67.9	29.3	2.3	0.5	16.9	0.1	5.8	1.4	184.4	0.2	0.7	398,553	37.4
	4	72.3	23.0	4.5	0.2	6.7	0.0	9.8	2.0	349.0	0.2	0.4	400,000	37.1
Site 4	1	74.7	23.4	1.7	0.1	4.0	0.1	11.6	2.9	330.1	0.3	0.3	398,439	37.0
	2	72.3	26.2	1.0	0.5	5.2	0.1	13.6	2.8	389.9	0.3	0.4	400,000	37.4
	3	74.1	24.8	0.7	0.4	3.4	0.1	14.5	2.8	384.2	0.3	0.3	400,000	37.1
	4	70.2	29.0	0.6	0.2	4.4	0.1	16.5	2.9	402.4	0.4	0.5	400,000	37.4
Site 1B	1	69.3	28.5	1.9	0.2	9.2	0.1	11.5	1.6	327.3	0.2	0.5	400,000	37.3
	2	68.6	29.7	1.4	0.3	10.2	0.1	11.3	1.6	333.6	0.2	0.5	400,000	37.3
	3*	43.4	53.8	1.2	1.6	38.8	1.3	8.1	2.0	496.9	0.2	21.2	400,000	37.7
	4	74.5	24.3	0.9	0.3	7.0	0.1	11.1	1.8	305.6	0.2	0.8	400,000	37.2
Site 5	1*	67.1	29.0	3.3	0.5	15.5	0.3	8.0	1.1	293.5	0.2	18.7	400,000	37.7
	2	71.5	26.0	2.3	0.2	4.2	0.1	13.7	1.2	386.5	0.2	3.3	400,000	37.3
	3	72.5	24.8	2.5	0.2	3.3	0.1	14.5	1.1	373.8	0.2	1.6	400,000	37.3
	4	71.0	27.0	1.8	0.1	4.7	0.1	14.0	1.2	391.4	0.2	0.8	400,000	37.4
Site 6	1	79.0	20.1	0.8	0.2	3.0	0.0	11.8	1.4	278.4	0.2	1.0	400,000	37.0
	2	76.7	22.6	0.5	0.2	5.8	0.0	10.8	1.4	286.0	0.1	1.0	392,922	36.5
	3	78.5	20.7	0.7	0.1	4.3	0.0	9.8	1.4	264.9	0.1	1.2	400,000	37.2
	4	77.7	21.6	0.5	0.1	4.3	0.1	11.6	1.4	290.4	0.1	1.0	395,841	37.2
Site 7	1	78.1	19.4	2.4	0.1	3.7	0.2	11.3	1.6	317.7	0.2	0.3	400,000	37.3
	2	81.5	16.1	2.3	0.1	3.0	0.2	9.4	1.6	260.1	0.1	0.3	400,000	37.2
	3	80.7	17.6	1.6	0.1	2.4	0.2	12.2	1.7	333.6	0.2	0.5	400,000	37.2

(Continues)

TABLE 3 (Continued)

Multi-site whole blood reproducibility study: Cleanup statistics[a]

Site	Replicate	%Clean[b]	%Excluded	%Beads[b]	%Unclass[c]	%Debris	%Dead	%Aggs	CeO$_2$ ratio	Acq rate	%CD19+ CD3+ [d]	%CD14+ CD3+ [e]	Total cells	Run time [f]
	4	83.0	15.7	1.2	0.1	2.5	0.2	10.7	1.7	304.6	0.1	0.4	400,000	37.2
Averages		70.9	26.9	1.8	0.4	9.0	0.2	10.9	1.7	326.8	0.2	2.6	399,507	37.3

All FCS files were automatically analyzed by the Cleanup model.
The %Clean column quantifies the percentage of total events that were exported without debris, dead cells, aggregates, and normalization beads. %Excluded are the non-bead excluded events and %Beads are the normalization bead percentage. %Unclass are the percentage of unclassified events. The %Clean+%Excluded+%Bead+%Unclass fields add to 100%. %Debris are the sub DNA1 events that are not beads, %Aggs are the high DNA1 events, and %Dead are the events that are Live/Dead+. CeO+ ratio is an indicator of plasma temperature and should be less than 3.0. The acquisition rate is the number of acquired events/s, which is recommended to be approximately 350 events/s. The %CD19 + CD3+ and %CD14 + CD3+ columns are indicators of cell aggregation and coincident ion clouds. Total Cells are the total number of events acquired for analysis, and Run Time is the length of time in seconds for cleanup analysis. Three files were excluded due to background signal in the Er168 channel.

or coincident ion clouds; 1.8% were normalization beads; and 0.4% were unclassified. Approximately 13.2% of the excluded events were debris, 10.9% were high DNA1 aggregates, and the %dead cell count was low at 0.2%. All files had CeO+ ratios, a measure of plasma temperature, of less than 3. The average acquisition rate was approximately 326.8 events/s, and the average % of aggregates was reasonably low (%CD19 + CD3+ and %CD14 + CD3+ less than 0.2 and 2.6%, respectively). A total of 400,000 events were considered by the cleanup routine, and the average time spent in this step was approximately 37 s.

The deep immunophenotyping frequency results for whole blood are summarized in Table 4. The left side of the table shows the enumerated populations, and the numbers indicate the percentages of live intact cells in each of the replicates from all seven sites. Three replicates (Site 1A Rep 4, Site 1B Rep 3, and Site 5 Rep 1) were excluded due to background signal in the Er168 channel (see Section 4 for details). Figure 3 summarizes the inter-site reproducibility of all populations with both SDs and %CV of each population. Means, SDs, and %CVs from Sites 1A, 2, 3, and 4 were calculated separately from Sites 1B, 5, 6, and 7 because they were from a different sample. Statistics from both sets of sites were averaged. The percentages of live intact cells for each population and SDs are summarized in the top panel, and the %CVs are presented as a bar graph in the bottom panel. The inter-site average %CV was 14.4%, ranging from 2.3 to 96.6%, with higher %CVs generally associated with very low-frequency populations. The intra-site reproducibility is summarized in Table 5 and had an average %CV of 7.9%.

3.2 | PBMC

A total of 24 FCS3.0 PBMC-derived files from six different sites were analyzed by the cleanup phase of the analysis (See Table 6 for a summary of the results). On average, 76.7% of the events were considered desirable "live intact cells"; 21.4% were excluded because they were classified as dead cells, debris, true aggregates, aborted pulses, or coincident ion clouds; 1.8% were normalization beads, and 0.08% were unclassified. Approximately 4.2% of the excluded events were debris, 0.9% were dead, and 11.4% were high DNA1 aggregates. All files had CeO+ ratios of less than 3.5. The average acquisition rate was approximately 300 events/s, and the average % of double-positive aggregates was reasonably low (%CD19 + CD3+ and % CD14 + CD3+ less than 0.3 and 2.3%, respectively). Approximately 300,000 events were considered by the cleanup routine, and the average time spent in this step was approximately 33 s.

The deep immunophenotyping results are summarized in Table 7. The left side of the table shows the enumerated populations, and the numbers indicate the percentages of live intact cells from the four replicates from all six sites. Figure 4 summarizes the inter-site reproducibility of the percentages with both SDs as well as %CV. The percentiles and SDs are summarized in the top panel, and the %CVs presented as a bar graph in the bottom panel. The percentages, SDs, and %CVs were an average of Cohort 1 (Week 1) and 2 statistics. The average and median %CV were 17.7 and 13.7%, respectively. The

TABLE 4 Multi-site whole blood reproducibility study

Whole blood reproducibility study: Population percentages[a]

Blood source	Donor week 1[b]															Same donor week 2[c]																
Site	Site 1A[d]			Site 2				Site 3				Site 4				Site 1B				Site 2				Site 6				Site 7			
Replicate	1[e]	2	3	1	2	3	4	1	2	3	4	1	2	3	4	1	2	3	4	1	2	3	4	1	2	3	4	1	2	3	4
Lymphocytes	28.2	27.8	29.4	25.7	27.3	26.2	28.2	24.9	26.7	24.7	25.5	27.1	26.9	25.6	27.0	22.1	22.1	22.1	21.2	18.3	19.4	20.3	18.0	21.5	20.3	20.3	19.3	22.4	22.4	20.8	22.3
CD3 T cells	19.9	19.4	20.5	18.0	19.0	18.3	19.6	17.7	18.6	17.4	18.4	19.2	18.9	17.6	19.1	15.7	15.5	15.1	14.8	12.8	13.9	14.4	12.7	15.2	14.3	14.4	13.7	15.9	15.9	15.1	15.8
CD8 T cells	4.4	4.3	4.6	4.1	4.3	4.1	4.5	4.1	4.3	4.0	4.2	4.5	4.4	4.2	4.4	3.3	3.3	3.3	3.1	2.8	3.0	3.0	2.8	3.3	3.0	3.1	2.9	3.5	3.5	3.3	3.5
CD8 naïve	2.7	2.6	2.8	2.6	2.6	2.6	2.8	1.9	2.3	2.0	2.4	2.7	2.6	2.5	2.6	2.0	2.0	2.0	1.9	1.7	1.8	1.8	1.7	2.0	1.8	1.8	1.7	2.0	2.1	2.0	2.1
CD8 central memory	0.6	0.5	0.6	0.4	0.4	0.4	0.4	0.9	0.8	0.7	0.5	0.6	0.5	0.5	0.5	0.4	0.3	0.3	0.3	0.3	0.3	0.3	0.3	0.3	0.3	0.3	0.3	0.4	0.3	0.3	0.3
CD8 effector memory	1.0	1.0	1.1	1.0	1.1	1.0	1.1	1.1	1.1	1.1	1.1	1.0	1.1	1.1	1.1	0.8	0.8	0.9	0.8	0.7	0.7	0.9	0.8	0.9	0.8	0.9	0.8	1.0	0.9	0.9	1.0
CD8 terminal effector	0.2	0.2	0.2	0.2	0.2	0.2	0.2	0.2	0.2	0.2	0.2	0.2	0.2	0.2	0.2	0.1	0.1	0.2	0.2	0.1	0.1	0.1	0.1	0.1	0.1	0.1	0.1	0.2	0.2	0.1	0.1
CD4 T cells	12.8	12.5	13.1	11.4	12.1	11.7	12.5	11.3	11.7	10.9	11.6	12.3	12.1	11.7	12.3	10.1	9.8	8.8	9.5	8.0	8.8	9.2	7.9	9.7	9.1	9.2	8.9	9.9	10.0	9.5	10.0
CD4 naïve	2.8	2.7	2.9	3.0	3.3	3.0	3.4	1.5	1.9	1.8	2.2	2.7	2.8	2.8	2.8	2.3	2.2	2.4	2.2	2.2	2.2	2.2	2.1	2.4	2.2	2.2	2.2	2.3	2.4	2.2	2.4
CD4 central memory	4.3	4.3	4.2	3.3	3.5	3.4	3.6	4.4	4.4	3.9	3.9	3.9	3.5	2.8	4.0	3.2	3.2	2.1	3.0	1.8	1.8	2.7	2.0	2.9	2.7	2.7	2.5	2.7	2.7	2.5	2.9
CD4 effector memory	4.5	4.4	4.8	4.0	4.2	4.1	4.4	4.3	4.2	4.2	4.4	4.5	4.7	5.1	4.3	3.6	3.5	3.4	3.4	3.2	3.2	3.4	3.2	3.4	3.2	3.4	3.7	3.8	3.9	3.8	3.7
CD4 terminal effector	1.1	1.1	1.2	1.1	1.2	1.1	1.1	1.0	1.2	1.1	1.1	1.2	1.1	1.0	1.2	1.0	0.9	0.9	1.0	0.8	0.8	0.9	0.9	1.0	0.9	0.9	0.9	1.1	1.0	1.0	1.0
γδ T cells	1.5	1.4	1.5	1.4	1.4	1.4	1.5	1.3	1.4	1.4	1.5	1.4	1.4	1.5	1.5	1.2	1.2	1.1	1.2	1.1	1.1	1.1	1.1	1.2	1.2	1.1	1.1	1.3	1.3	1.2	1.2
MAIT/NKT cells	1.2	1.2	1.2	1.1	1.1	1.1	1.1	1.0	1.1	1.1	1.1	1.0	1.0	0.2	0.9	1.2	1.1	1.0	1.0	1.0	1.0	1.0	1.0	1.0	0.9	1.0	0.9	1.1	1.2	1.1	1.1
B cells	3.6	3.5	3.8	2.9	3.2	3.0	3.4	2.2	3.0	2.2	1.6	3.0	2.9	3.0	2.8	2.4	2.5	2.0	2.3	1.7	1.7	1.8	1.7	2.0	1.9	1.8	1.7	2.3	2.2	2.0	2.2
B Naïve	3.2	3.1	3.4	2.6	2.8	2.7	3.1	1.9	2.6	1.9	1.4	2.7	2.5	2.6	2.5	2.1	2.2	1.8	2.1	1.5	1.5	1.5	1.5	1.7	1.7	1.5	1.5	2.0	2.0	1.8	2.0
B memory	0.3	0.4	0.4	0.3	0.3	0.3	0.3	0.3	0.3	0.3	0.2	0.3	0.3	0.3	0.3	0.2	0.2	0.3	0.2	0.2	0.2	0.3	0.2	0.2	0.2	0.2	0.2	0.2	0.2	0.2	0.2
Plasmablasts	0.0	0.0	0.0	0.0	0.0	0.0	0.0	0.0	0.0	0.0	0.0	0.0	0.0	0.0	0.0	0.0	0.0	0.0	0.0	0.0	0.0	0.0	0.0	0.0	0.0	0.0	0.0	0.0	0.0	0.0	0.0
NK cells	4.7	4.9	5.1	4.8	5.1	4.9	5.2	5.0	5.2	5.0	5.4	4.9	5.1	5.0	5.1	4.1	4.1	3.5	4.0	3.7	3.7	4.1	3.6	4.3	4.1	4.1	3.9	4.3	4.2	3.7	4.2
NK early	3.9	4.0	4.3	3.7	4.0	3.8	4.1	4.4	4.5	4.4	4.7	3.9	4.0	4.0	4.0	3.4	3.4	2.7	3.3	2.8	2.8	3.3	3.1	3.5	3.4	3.3	3.2	3.3	3.2	2.8	3.2
NK late	0.8	0.8	0.9	1.0	1.1	1.1	1.1	0.6	0.6	0.7	0.7	1.1	1.1	1.0	1.1	0.7	0.7	0.8	0.7	0.9	0.8	0.8	0.9	0.8	0.8	0.8	0.8	1.0	1.0	0.9	1.0
Monocytes	3.6	3.7	3.8	4.0	3.8	3.8	3.9	2.7	3.0	2.8	2.6	3.2	2.6	1.9	2.5	3.0	3.1	4.4	3.3	2.6	2.6	4.6	4.0	4.2	4.4	4.6	4.4	4.6	4.8	4.8	4.7
Monocytes classical	3.2	3.3	3.4	3.5	3.4	3.6	3.5	2.0	2.4	2.1	2.2	2.8	2.1	1.5	2.1	2.7	2.9	4.1	3.0	2.3	2.3	4.2	3.7	3.8	4.0	4.2	4.1	4.3	4.4	4.5	4.4
Monocytes Intermediate	0.2	0.2	0.3	0.2	0.2	0.2	0.2	0.4	0.4	0.4	0.2	0.2	0.2	0.2	0.2	0.1	0.2	0.1	0.2	0.1	0.1	0.2	0.2	0.2	0.2	0.2	0.2	0.2	0.2	0.1	0.2
Monocytes nonclassical	0.2	0.2	0.2	0.2	0.2	0.2	0.2	0.3	0.3	0.3	0.2	0.2	0.2	0.2	0.2	0.1	0.1	0.2	0.1	0.1	0.1	0.2	0.1	0.2	0.2	0.1	0.2	0.2	0.2	0.1	0.2
DCs	0.3	0.5	0.3	0.2	0.2	0.2	0.3	0.3	0.4	0.5	0.3	0.2	0.3	0.2	0.3	0.2	0.2	0.3	0.2	0.3	0.3	0.2	0.3	0.2	0.2	0.2	0.2	0.2	0.2	0.2	0.2
pDCs	0.1	0.1	0.1	0.1	0.1	0.1	0.1	0.1	0.1	0.1	0.1	0.1	0.1	0.1	0.1	0.1	0.1	0.1	0.1	0.1	0.1	0.1	0.1	0.1	0.1	0.1	0.1	0.1	0.1	0.1	0.1
mDCs	0.2	0.4	0.2	0.2	0.2	0.1	0.2	0.2	0.1	0.4	0.2	0.1	0.2	0.2	0.2	0.2	0.2	0.2	0.2	0.2	0.2	0.2	0.2	0.2	0.2	0.2	0.1	0.1	0.1	0.2	0.2
Granulocytes	64.1	64.3	63.1	65.3	63.6	65.8	63.4	65.4	64.4	66.9	66.3	65.3	66.4	66.4	66.6	71.2	70.8	70.8	70.9	74.2	72.7	71.5	74.6	70.8	71.0	71.5	73.0	69.0	68.7	70.2	69.1
Neutrophils	61.7	62.1	61.0	63.3	61.8	63.8	61.6	62.7	60.9	63.8	63.9	61.2	63.1	59.3	61.9	69.4	68.9	68.9	68.7	72.3	70.5	69.9	72.8	69.0	69.2	69.9	71.0	67.4	67.1	68.6	67.5

(Continues)

TABLE 4 (Continued)

Whole blood reproducibility study: Population percentages[a]

Blood source	Donor week 1[b]																			Same donor week 2[c]											
Site	Site 1A[d]			Site 2				Site 3				Site 4				Site 1B				Site 2				Site 6				Site 7			
Replicate	1[e]	2	3	1	2	3	4	1	2	3	4	1	2	3	4	1	2	3	4	1	2	3	4	1	2	3	4	1	2	3	4
Basophils	0.7	0.7	0.8	0.7	1.0	0.7	0.7	0.7	0.7	0.7	0.7	0.6	0.7	0.6	0.6	0.6	0.7	0.6	0.6	0.6	0.5	0.6	0.6	0.5	0.6	0.6	0.6	0.7	0.7	0.6	0.6
Eosinophils	1.1	1.0	0.8	1.1	1.0	1.1	1.0	0.9	0.9	1.1	0.9	1.0	1.0	1.5	0.7	0.9	0.9	1.0	1.0	0.9	0.9	0.9	1.0	1.0	1.0	1.0	1.0	0.9	0.9	1.0	1.0
CD66b- Neuts	0.6	0.5	0.6	0.4	0.1	0.2	0.1	0.2	0.2	1.5	0.4	2.6	1.6	5.7	3.2	0.4	0.4	0.1	0.1	0.4	0.5	0.7	0.6	0.3	0.2	0.3	0.1	0.0	0.0	0.0	0.0
Tregs	0.4	0.4	0.4	0.4	0.4	0.4	0.4	0.2	0.2	0.2	0.3	0.3	0.3	0.3	0.3	0.4	0.3	0.3	0.3	0.3	0.3	0.3	0.3	0.3	0.3	0.3	0.3	0.3	0.3	0.3	0.3
Th1-like	0.9	1.0	1.0	0.7	0.9	0.8	0.9	1.3	1.3	1.0	1.1	1.0	1.1	1.0	1.1	0.7	0.7	0.7	0.7	0.7	0.6	0.7	0.7	0.7	1.2	0.7	0.7	0.7	0.7	0.7	0.7
Th2-like	0.9	0.8	0.9	0.7	0.7	0.7	0.7	1.0	1.1	0.8	0.8	0.8	0.8	0.8	0.6	0.7	0.7	0.6	0.6	0.7	0.5	0.6	0.5	0.6	0.9	0.6	0.5	0.7	0.7	0.6	0.7
Th17-like	0.6	0.6	0.7	0.6	0.6	0.6	0.6	0.3	0.4	0.6	0.6	0.6	0.6	0.6	0.5	0.6	0.5	0.5	0.5	0.6	0.4	0.4	0.4	0.5	0.2	0.5	0.5	0.5	0.6	0.6	0.5

The above table summarizes all the frequency results for all sites and populations in terms of percent live intact cells.

[a] All samples were stained with Maxpar Direct Immune Profiling Assay.

[b] Same donor of whole blood sent to left four test sites.

[c] Same donor was drawn in week two and sent to right four test sites.

[d] Four replicates per site were processed except for three files with high background in 163Er channel (see Section 4).

[e] Population percentages are of intact live cells.

FIGURE 3 Whole blood reproducibility. The top panel shows the mean and ± *SD* percentage of live intact cells for all 37 evaluated populations across all seven sites. The bottom panel shows the associated %CVs for each population where the average was 14.4% [Color figure can be viewed at wileyonlinelibrary.com]

intra-site reproducibility is summarized in Table 8 and had an average and median %CV of 8.4 and 4.5%, respectively, for all sites and populations.

4 | DISCUSSION

The average event inclusion percentage for this study was approximately 70% for whole blood (see Table 3) and 76.7% for PBMC (see Table 6), which are generally comparable to gate-based inclusion percentages (data not shown). The site-to-site variability is probably either due to different environmental factors during the shipping of the samples or to slightly different site specimen handling techniques. The increase in %CD14+ CD3+ in Table 3 is due to the inclusion of the three files with a high CD14 Er168 background.

The average acquisition rate for both the whole blood and PBMC studies was approximately 300 events/s. Although the acquisition system can be set for faster rates, the Poisson nature of ion cloud formation creates more coincident clouds at faster rates. Most of these coincident events are removed in the cleanup stage, but the routine is not 100% effective in eliminating these events. A rate between 250 and 350 events/s is currently recommended by Fluidigm (Fluidigm, 2018).

The Cleanup model exports FCS3.0 data that are not only available for PSM automated analysis but also for other types of cytometry analysis as well. For investigators interested in oncological samples, the DNA selection parts of the Cleanup model can easily be deactivated in order that DNA hyperdiploid populations are not

TABLE 5 Whole blood intra-site reproducibility

Whole blood intra-site reproducibility %CV										
Population	Site 1A	Site 2	Site 3	Site 4	Average Wk 1	Site 1B	Site 5	Site 6	Site 7	Average Wk 2
Lymphocytes	2.8	4.1	4.0	1.5	3.1	2.4	8.3	5.2	4.2	4.0
CD3 T cells	2.6	3.7	3.1	2.2	2.9	2.9	8.4	6.0	2.8	3.9
CD8 T cells	3.3	3.5	3.7	3.1	3.4	3.6	6.5	7.9	2.6	4.2
CD8 naïve	3.5	4.0	7.8	3.8	4.8	4.3	8.4	7.0	2.6	5.1
CDS central memory	4.9	5.0	18.5	8.4	9.2	6.0	5.3	12.4	2.8	8.0
CDS effector memory	2.5	4.5	1.9	3.7	3.1	2.7	4.0	9.9	4.4	4.1
CDS terminal effector	3.7	4.1	6.8	9.7	6.1	12.0	9.7	6.4	8.7	7.5
CD4 T cells	2.6	4.0	3.0	1.9	2.9	2.9	10.3	4.7	2.9	3.9
CD4 naïve	4.1	5.7	17.7	2.1	7.4	2.0	7.1	2.9	3.8	5.9
CD4 central memory	3.3	4.5	7.4	15.3	7.6	8.0	23.3	3.9	7.5	9.0
CD4 effector memory	4.2	4.8	0.6	8.6	4.6	2.2	6.0	6.3	1.7	4.3
CD4 terminal effector	9.4	6.1	4.2	7.3	6.7	3.6	8.1	10.6	1.4	6.4
γδ T cells	3.9	3.8	4.7	3.1	3.9	1.5	5.9	7.3	4.3	4.3
MAIT/NKT cells	3.4	1.9	2.4	10.9	4.6	4.0	2.6	12.0	4.1	5.1
B cells	4.0	6.5	23.5	1.9	9.0	3.1	11.8	12.5	5.7	8.7
B naïve	4.4	6.6	25.4	2.0	9.6	2.6	10.7	13.6	5.9	9.0
B memory	2.8	6.9	12.8	3.9	6.6	7.0	20.6	8.5	5.0	8.2
Plasmablasts	11.3	9.7	15.5	21.7	14.5	10.3	16.3	15.8	11.7	14.1
NK cells	4.3	4.1	8.5	1.7	4.6	1.6	9.0	3.2	9.4	5.2
NK early	4.3	5.0	7.0	1.9	4.6	2.1	12.6	5.8	10.1	5.9
NK late	4.5	1.5	19.6	4.0	7.4	0.9	6.9	8.8	7.5	6.8
Monocytes	2.7	1.9	4.2	10.7	4.9	5.4	21.2	2.0	1.1	6.0
Monocytes classical	2.7	2.0	3.6	13.5	5.5	5.6	22.2	2.8	1.2	6.6
Monocytes transitional	4.4	9.3	29.5	7.9	12.8	6.8	10.6	16.5	2.7	11.2
Monocytes non-classical	5.2	5.8	13.1	6.6	7.7	2.4	19.5	7.5	8.7	8.5
DCs	35.0	7.9	21.4	16.7	20.3	5.4	8.5	4.7	4.7	13.8
pDCs	5.8	3.0	9.7	1.6	5.0	11.0	15.0	9.6	7.0	7.5
mDCs	43.4	11.9	26.3	24.1	26.4	3.2	6.1	6.1	3.7	16.8
Granulocytes	1.2	1.9	1.6	0.8	1.4	0.2	2.6	2.1	1.2	1.4
Neutrophils	1.0	l.8	2.1	2.6	1.9	0.5	2.5	2.1	1.2	1.7
Basophils	5.6	2.6	1.5	7.9	4.4	4.3	6.5	7.0	1.9	4.6
Eosinophils	14.4	3.8	3.5	4.1	6.5	2.0	5.5	3.1	2.6	5.1
CD66b- Neuts	8.6	73.7	38.9	53.2	43.6	36.6	35.9	66.1	37.4	43.8
Tregs	5.0	2.6	25.1	3.7	9.1	5.6	7.0	4.5	4.6	7.5
Th1-like	2.9	7.0	6.4	4.9	5.3	5.9	8.6	30.0	6.2	8.6
Th2-like	3.9	4.0	5.2	5.2	4.6	7.0	11.0	19.3	7.6	7.5
Th17-like	4.9	5.6	14.5	1.9	6.7	3.8	13.2	29.9	3.9	9.4
Mean	6.4	6.6	10.9	7.7	7.9	5.2	10.7	10.4	5.5	7.9

removed. However, if these measurements are deactivated, the number of true aggregates in the exported "cleaned" file is likely to increase. The data obtained in the multi-site study were generated using a prototype panel lot. Three out of 24 runs were excluded from the data presented due to background signals in the Er168 channel, which has been eliminated in subsequent manufacturing lots.

The staging approach for CD8 T-cells (see Table 2) was to first model the downregulation of CCR7 and CD27 to stratify events into three compartments: naïve + central memory, effector memory, and terminal effector. CD45RA was found not to be a good modeling marker for staging because of its relatively wide line-spread (data not shown) and branched nature (Inokuma, Maino, & Bagwell, 2013). The

TABLE 6 PBMC cleanup summary statistics

		% Clean [b]	% Excluded	% Beads	% Unclass [c]	% Debris	% Dead	% Aggs	CeO₂ ratio	Acq rate	%CD19+ CD3+ [d]	%CD14+ CD3+ [e]	Total Cells	Run time [f]
Multi-site PBMC reproducibility study: Cleanup statistics[a]														
Sites	Replicates													
Site 2	1	76.9	21.7	1.4	0.1	4.0	0.3	11.4	1.8	316.5	0.3	1.2	300,000	32.2
	2	75.9	22.8	1.3	0.1	5.2	0.3	11.1	1.9	298.8	0.3	1.4	300,000	33.2
	3	77.3	21.5	1.1	0.1	4.1	0.2	11.1	1.9	313.2	0.3	1.1	300,000	33.0
	4	78.2	20.5	1.3	0.1	4.3	0.2	10.1	1.2	214.2	0.2	1.1	288,975	32.4
Site 3	1	73.7	24.0	2.2	0.1	6.8	0.1	11.4	2.1	266.1	0.4	1.3	298,335	33.1
	2	68.8	28.4	2.6	0.1	8.7	0.1	13.2	2.1	303.5	0.5	1.6	400,000	39.9
	3	76.6	16.7	6.6	0.1	3.0	0.1	7.8	2.0	248.3	0.2	1.2	300,000	33.6
	4	75.2	19.4	5.3	0.1	4.0	0.1	9.0	2.0	279.3	0.3	1.9	300,000	32.9
Site 4	1	72.1	27.0	0.8	0.1	6.2	0.6	15.0	2.8	413.2	0.6	1.5	300,000	33.7
	2	66.4	32.6	0.7	0.2	6.2	0.4	18.2	3.3	414.9	0.5	1.6	300,000	33.3
	3	79.2	19.5	1.2	0.1	4.0	0.3	10.6	3.0	300.0	0.4	1.4	300,000	32.5
	4	76.7	21.7	1.5	0.1	5.1	0.2	11.3	2.9	295.6	0.5	1.5	300,000	32.8
Site 5	1	75.7	22.8	1.4	0.1	2.2	0.2	15.5	1.1	403.8	0.5	1.4	300,000	32.9
	2	78.2	20.0	1.7	0.1	2.0	0.0	13.5	1.1	361.0	0.4	1.3	300,000	32.6
	3	75.9	22.5	1.5	0.1	2.8	0.2	15.2	1.2	394.7	0.4	7.9	300,000	32.7
	4	77.4	20.2	2.2	0.2	8.2	0.4	7.6	1.2	241.5	0.2	14.2	300,000	32.5
Site 6 [g]	1	75.6	23.3	1.0	0.1	4.6	3.1	11.0	1.4	254.2	0.2	1.2	300,000	33.0
	2	74.4	24.9	0.6	0.1	6.1	3.6	10.2	1.4	244.7	0.3	1.9	297,593	32.6
	3	83.6	15.3	1.1	0.0	2.5	2.8	5.4	1.4	127.6	0.1	2.0	300,000	32.8
	4	75.7	19.5	4.7	0.1	4.9	4.0	6.5	1.4	164.5	0.2	2.3	300,000	32.4
Site 7	1	81.7	17.4	0.8	0.0	1.9	1.3	11.7	1.7	317.1	0.3	1.3	300,000	32.9
	2	80.7	18.6	0.7	0.0	1.7	1.6	12.9	1.6	356.7	0.3	2.0	300,000	33.0
	3	82.0	17.4	0.6	0.0	1.4	1.0	12.4	1.7	339.4	0.4	1.8	295,265	33.0
	4	83.5	15.9	0.6	0.0	1.4	0.9	11.1	1.9	308.3	0.3	1.7	300,000	32.7
Mean		76.7	21.4	1.8	0.08	4.2	0.9	11.4	1.8	299.1	0.3	2.3	303,340	33.2

[a]All samples were stained with Maxpar Direct Immune Profiling Assay.
[b]Percent of total events. %Cleaned+%Excluded+%Beads+%Unclassified = 100.
[c]Percent of events that were not classified into the cell types Cleaned, Excluded, or Beads.
[d]Percent of CD19+ CD3+ double positives of CD19+ singlets + CD3+ singlets.
[e]Percent of CD14+ CD3+ double positives of CD14+ singlets + CD3+ singlets.
[f]Units of seconds.
[g]The first acquisition of Site 6 samples had insufficient EQ Beads for normalization. Samples were spun down and resuspended again in fresh CAS/0.1 EQ Beads to acquire data for analysis.

system then used a combinatory analysis system called TriCOM to divide the first stage into its naïve and central memory components. The staging approach for CD4 T-cells (see Table 2) was to model the downregulation of CD45RA, CCR7, and CD27 to create the four stages: naïve, central memory, effector memory, and terminal effector. The CD4 T-cell terminal effector was assumed to be CD45RA− because CD45RA+ events were generally not observed in any sample in this study (see Figure 5) and it has been recognized that there are a few if any CCR7− CD45RA+ events in the CD4 T-cell compartment for healthy individuals (Seder & Almed, 2003).

Subclassification of monocytes into Classical, Transitional, and Non-classical used CD14 and CD38 (see Table 2) instead of the more traditional CD14 and CD16 (Picozza, Battistini, & Borsellino, 2013). The patterns produced by CD14 and CD38 were found to classify analogous subpopulations while improving the overall reproducibility of the results (data not shown).

The data presented in Tables 4 and 7 summarize all the cell population frequency results obtained from the whole blood and PBMC studies. An inspection of these tables shows the high degree of reproducibility of the system for almost all immune populations. Figures 3 and 4 summarize the inter-site variability of the whole blood and PBMC studies. The populations are ordered from the highest percentage (left) to the lowest (right) in order to better appreciate the general effect of counting error increasing the magnitude of CVs for

TABLE 7 Multi-site PBMC reproducibility study

Multi-site PBMC reproducibility study: Population percentages[a]

Site	Site 2 [b]				Site 3				Site 4				Site 5				Site 6				Site 7			
Replicate	1 [c]	2	3	4	1	2	3	4	1	2	3	4	1	2	3	4	1	2	3	4	1	2	3	4
Lymphocytes	67.1	65.9	66.4	65.7	67.0	67.5	67.4	67.2	65.6	65.7	66.0	66.0	75.6	73.6	65.5	62.4	64.3	64.3	70.1	62.7	68.1	68.3	69.4	69.8
CD3 T cells	50.5	49.8	50.1	50.1	48.6	49.6	48.0	48.4	48.0	47.7	46.1	44.9	50.8	51.6	46.2	40.1	48.6	48.5	46.4	43.5	48.2	48.6	50.6	50.3
CD8 T cells	10.3	10.1	10.2	10.1	10.3	10.4	10.2	10.2	10.3	10.2	10.4	10.3	11.4	11.2	9.8	9.8	10.6	10.6	12.6	10.4	10.6	10.2	10.5	10.5
CD8 naïve	6.2	6.1	6.2	6.1	6.0	6.0	5.9	5.9	6.2	6.4	6.3	6.2	6.2	6.4	5.9	5.3	6.4	6.4	7.4	6.0	6.2	5.8	6.1	5.9
CD8 central memory	0.4	0.4	0.5	0.5	0.5	0.6	0.6	0.6	0.6	0.4	0.5	0.5	0.5	0.4	0.4	0.2	0.5	0.5	0.4	0.4	0.3	0.4	0.4	0.4
CD8 effector memory	2.0	2.1	2.0	2.0	2.2	2.2	2.0	2.1	1.7	1.5	1.7	1.6	2.6	2.5	2.0	2.3	1.9	1.8	2.1	1.9	2.3	2.3	2.2	2.4
CD8 terminal effector	1.6	1.4	1.5	1.6	1.7	1.6	1.7	1.6	1.7	1.8	1.9	2.0	2.2	1.9	1.5	2.0	1.9	1.9	2.7	2.0	1.9	1.8	1.8	1.9
CD4 T cells	32.4	32.0	32.1	32.3	29.9	30.8	29.5	30.0	31.5	31.1	29.2	28.4	29.8	30.7	28.6	23.9	29.7	29.8	24.5	25.4	30.4	30.3	31.6	31.2
CD4 naïve	12.7	12.5	12.4	12.6	11.1	11.4	11.0	11.3	13.5	13.8	12.3	12.6	12.8	13.3	12.7	10.2	11.4	12.2	11.3	9.9	12.4	12.6	13.0	12.6
CD4 central memory	6.4	6.3	7.0	6.5	6.6	6.7	6.7	6.9	6.7	6.1	5.9	5.5	4.4	4.9	4.7	3.3	6.8	6.4	4.1	5.6	5.6	5.1	5.5	5.3
CD4 effector memory	9.8	9.8	9.2	9.7	8.4	8.4	7.9	7.8	6.5	6.6	6.6	6.0	9.0	8.7	8.1	7.2	7.3	7.1	5.3	6.0	8.3	8.6	9.1	9.1
CD4 terminal effector	3.5	3.5	3.6	3.5	3.8	4.3	3.9	4.1	4.8	4.6	4.4	4.2	3.7	3.8	3.1	3.3	4.1	4.2	3.8	3.9	4.1	3.9	4.0	4.1
γδ T cells	4.3	4.4	4.3	4.2	4.6	4.7	4.5	4.6	4.4	4.4	4.5	4.5	6.0	5.3	4.4	4.5	4.4	4.5	5.4	4.6	4.8	4.5	4.6	4.7
MAIT/NKT cells	3.5	3.3	3.5	3.5	3.7	3.7	3.8	3.6	1.8	1.9	1.9	1.8	3.6	4.4	3.3	1.8	4.0	3.6	4.0	3.1	2.4	3.6	3.9	4.0
B cells	7.1	6.6	6.9	6.4	7.6	7.6	8.0	8.0	7.9	8.1	8.6	9.1	8.5	8.0	7.4	6.2	5.3	5.2	5.1	5.8	7.4	7.3	7.3	7.3
B naïve	5.9	5.4	5.6	5.3	6.4	6.4	6.8	6.7	6.7	6.7	7.3	7.8	7.3	6.9	6.3	5.3	4.3	4.3	4.3	4.8	6.3	6.2	6.1	6.2
B memory	1.1	1.1	1.1	1.0	1.1	1.1	1.1	1.2	1.2	1.3	1.3	1.3	1.1	1.0	1.0	0.7	0.9	0.8	0.7	0.9	1.0	1.0	1.0	1.0
Plasmablasts	0.1	0.1	0.1	0.1	0.1	0.1	0.1	0.1	0.1	0.1	0.1	0.1	0.1	0.1	0.1	0.1	0.1	0.1	0.1	0.1	0.1	0.1	0.1	0.1
NK cells	9.6	9.5	9.4	9.1	10.8	10.3	11.4	10.9	9.6	10.0	11.3	11.9	16.4	14.1	11.9	16.2	10.3	10.6	18.6	13.4	12.5	12.3	11.6	12.2
NK early	2.7	2.7	2.7	2.7	3.5	3.4	3.8	3.5	2.9	3.0	3.3	3.6	4.5	3.9	3.1	4.2	3.2	3.3	6.0	4.3	3.6	3.6	3.3	3.5
NK late	6.8	6.8	6.7	6.4	7.3	6.9	7.6	7.3	6.7	7.0	8.0	8.4	11.9	10.2	8.8	12.0	7.1	7.3	12.6	9.1	8.9	8.7	8.3	8.7
Monocytes	24.2	24.6	24.9	24.0	24.3	22.8	25.2	24.9	25.3	25.9	26.0	25.9	15.7	17.3	18.0	14.0	25.5	25.0	21.4	26.0	22.1	22.1	21.1	21.1
Monocytes classical	19.4	19.4	19.9	19.0	19.6	18.2	20.5	20.1	19.0	19.4	19.4	19.2	11.5	13.4	14.6	11.1	19.4	18.9	14.8	19.7	17.8	17.8	17.0	16.9
Monocytes transitional	2.9	3.1	2.9	2.9	2.7	2.6	2.8	2.9	3.3	3.0	3.3	3.3	2.1	2.3	2.8	2.5	3.5	3.4	3.0	3.4	2.6	2.6	2.5	2.5
Monocytes non-classical	1.9	2.1	2.0	2.1	1.9	1.9	1.9	1.9	3.1	3.4	3.3	3.3	2.1	1.7	1.7	0.4	2.6	2.6	3.6	2.9	1.7	1.7	1.6	1.7
DCs	0.9	0.9	0.9	0.8	1.0	1.0	0.9	0.8	1.0	1.2	1.0	1.0	0.7	0.7	0.3	0.2	1.3	1.3	1.5	1.2	1.1	1.0	0.9	1.0
pDCs	0.2	0.2	0.2	0.2	0.2	0.2	0.2	0.2	0.2	0.2	0.2	0.2	0.2	0.2	0.1	0.0	0.2	0.2	0.3	0.2	0.2	0.2	0.2	0.2
mDCs	0.7	0.7	0.7	0.7	0.9	0.9	0.7	0.6	0.8	1.0	0.8	0.7	0.6	0.6	0.2	0.1	1.1	1.1	1.3	1.0	0.9	0.8	0.8	0.8
Tregs	0.8	0.8	0.8	0.8	0.7	0.8	0.7	0.8	0.5	0.5	0.5	0.5	0.6	0.6	0.6	0.4	0.4	0.0	0.4	0.5	0.7	0.7	0.7	0.7
Th1-like	2.0	1.8	2.0	1.9	1.4	1.3	1.4	1.4	1.1	1.1	1.2	1.4	1.9	1.8	1.6	1.0	0.4	0.0	0.3	0.3	0.3	0.3	0.3	0.2

(Continues)

TABLE 7 (Continued)

Multi-site PBMC reproducibility study: Population percentages[a]

Site	Site 2 [b]				Site 3				Site 4				Site 5				Site 6				Site 7			
Replicate	1 [c]	2	3	4	1	2	3	4	1	2	3	4	1	2	3	4	1	2	3	4	1	2	3	4
Th2-like	2.1	2.2	2.1	2.2	2.9	3.2	2.8	3.0	3.1	2.9	2.8	3.0	3.8	4.0	3.7	3.3	5.6	0.0	3.0	4.5	5.2	5.1	5.0	4.1
Th17-like	2.6	2.7	2.6	2.7	2.9	3.0	2.8	2.9	2.5	2.4	2.1	1.5	1.7	1.8	1.6	1.5	0.3	5.7	0.7	0.4	1.6	1.6	2.1	3.1

The above table summarizes all the frequency results for all sites and populations in terms of percent live intact cells.

[a]All samples were stained with Maxpar Direct Immune Profiling Assay.

[b]Four replicates per site were processed.

[c]Population percentages are of live intact cells.
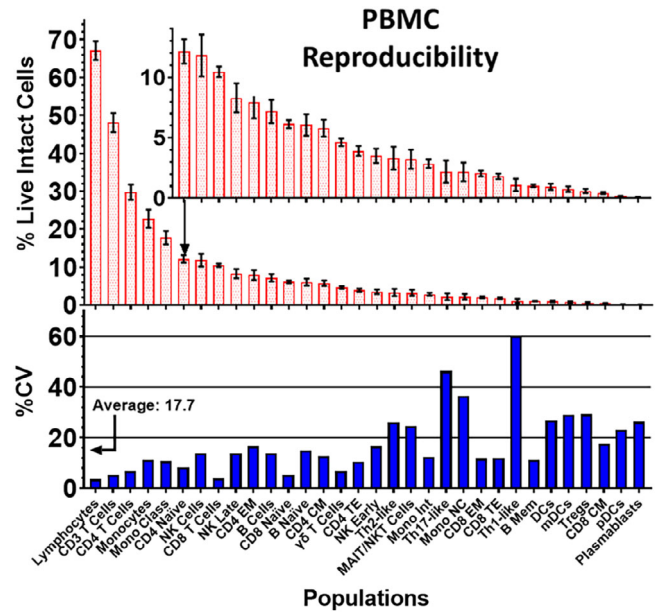
FIGURE 4 Peripheral blood mononuclear cells (PBMC) reproducibility. The top panel shows the mean and ±*SD* percentage of live intact cells for all 37 evaluated populations. Absent from this plot are the granulocyte, neutrophils, basophils, eosinophils, and CD66b− granulocytes. The bottom panel shows the associated %CVs for each population, where the average was 17.7%. The percentages, *SD*s, and %CVs were an average of Cohort 1 (Week 1) and 2 statistics [Color figure can be viewed at wileyonlinelibrary.com]

low-frequency populations. The average %CV for all 37 populations was 14.4% for whole blood and 17.7% for PBMC. The slight increase in variability for the PBMC may be due in part to the extra cell manipulations for this type of preparation. A high %CV was observed for the population labeled as CD66b− neutrophils in whole blood mainly due to its low frequency.

The upper panel insets with the ±*SD* ranges show a high degree of reproducibility even among many of the very low-frequency populations. Some populations are better defined by the panel than others, which explain some of the variability in the %CVs for populations with similar frequencies, and additional markers may be included to enhance identification in studies focused on low-frequency cell populations. The PBMC portion of this study is reasonably comparable to the multi-site study published by Leipold et al. (2018).

Tables 5 and 8 summarize the intra-site reproducibility of the whole blood and PBMC studies. As expected, the average and median intra-site %CV's are lower than the inter-site %CV's due to slight site-to-site biases. Some of the high intra-site %CV's for both whole blood and PBMC were due to outliers in the relatively small number of replicates. There was some disparity in intra-site %CV's across all populations among the sites in the study, which was more pronounced for low-frequency cell types.

The dry nature of the reagent in this assay eliminates most pipetting errors and reduces overall preparation time. An important feature of this system is that additional reagents can be added to

TABLE 8 PBMC intra-site reproducibility

Intra-site PBMC reproducibility %CV								
Population	Site 2	Site 3	Site 4	Site 5	Site 6	Site 7	Average	Median
Lymphocytes	1.0	0.3	0.3	9.1	5.0	1.2	2.8	1.1
CD3 T cells	0.5	1.4	3.1	11.2	5.1	2.4	4.0	2.7
CD8 T cells	0.9	1.3	0.9	8.2	9.2	1.6	3.7	1.4
CD8 naïve	1.0	0.7	1.6	8.0	9.0	2.6	3.8	2.1
CD8 central memory	10.0	4.6	13.5	25.8	13.4	18.3	14.3	13.4
CD8 effector memory	3.2	4.8	5.0	11.4	5.0	2.8	5.4	4.9
CD8 terminal effector	5.4	1.7	5.6	13.7	19.2	2.4	8.0	5.5
CD4 T cells	0.5	1.9	5.0	10.6	10.3	2.0	5.1	3.5
CD4 naïve	1.0	1.5	5.4	11.2	8.6	2.0	5.0	3.7
CD4 central memory	4.7	1.6	8.0	16.8	20.6	3.9	9.3	6.4
CD4 effector memory	3.2	3.9	4.4	9.6	14.8	4.1	6.7	4.3
CD4 terminal effector	1.2	5.7	5.3	9.6	5.1	2.1	4.8	5.2
γδ T cells	2.0	1.2	0.9	14.6	9.9	2.5	5.2	2.3
MAIT/NKT cells	2.1	2.3	3.1	32.8	11.3	20.9	12.1	7.2
B cells	4.3	2.9	6.4	13.2	5.7	0.6	5.5	5.0
B naïve	4.7	3.1	7.4	13.3	5.6	1.2	5.9	5.1
B memory	2.8	3.9	4.2	18.0	13.6	3.0	7.6	4.1
Plasmablasts	3.7	12.4	13.2	27.0	13.2	5.7	12.5	12.8
NK cells	2.3	4.0	10.1	14.4	29.0	3.3	10.5	7.0
NK early	0.9	4.6	9.4	14.8	30.4	3.8	10.7	7.0
NK late	3.0	3.8	10.4	14.3	28.4	3.1	10.5	7.1
Monocytes	1.6	4.4	1.2	11.0	8.5	2.5	4.9	3.5
Monocytes classical	1.8	5.0	1.1	12.9	12.6	2.6	6.0	3.8
Monocytes transitional	2.6	4.5	4.1	12.0	6.8	1.8	5.3	4.3
Monocytes non-classical	3.8	1.2	4.3	65.3	15.6	2.6	15.5	4.0
DCs	4.3	10.9	10.3	61.5	9.5	7.2	17.3	9.9
pDCs	0.2	5.2	5.6	60.7	13.1	4.7	14.9	5.4
mDCs	5.4	14.3	13.1	61.9	9.4	8.7	18.8	11.3
Tregs	2.7	3.3	8.0	13.5	58.6	4.9	15.2	6.5
Th1-like	5.3	5.6	12.1	24.8	66.7	18.6	22.2	15.3
Th2-like	2.4	4.5	3.9	8.2	73.8	10.6	17.2	6.4
Th17-like	1.9	2.8	20.4	8.1	146.3	33.8	35.6	14.3
Mean	2.8	4.0	6.5	20.2	21.7	5.9	10.2	6.2
Median	2.5	3.8	5.4	13.4	11.9	2.9	6.7	4.6

The 37 tested populations appear in the first column, and the %CVs of the four replicate PBMC samples are summarized for each site. The means and medians of the %CVs for all populations and sites appear on the outside rows and columns.

evaluate new populations because there are numerous open heavy metal channels. The Maxpar Pathsetter software is also designed for users to easily amend the models to take advantage of new markers and cell types.

The performance of the analysis system was designed to do a full and automated analysis in less than 5 min. The Cen-se′ mapping system is a high-resolution and highly parallelized variant of the t-SNE algorithm (van der Maaten, 2009, 2014; van der Maaten & Hinton, 2008) that can create maps of hundreds of thousands of events in 1 min or less.

The dry nature of the reagent coupled with automated data analysis is not only convenient but also provides a high degree of reproducibility within and among multiple test sites, whether they are analyzing whole blood or PBMC samples. This new mass cytometry assay provides a comprehensive yet practical solution for deep immune phenotyping.

CONFLICT OF INTEREST

Authors Bagwell, Hunsberger, Hill, Herbert, Bray, Selvanantham, Li, Inokuma, Goldberger, and Stelzer are currently employed or were employed by either Verity Software House or Fluidigm Corporation. Author Inokuma is a consultant for both Verity Software House and Fluidigm Corporation. This manuscript describes a component of the product, Fluidigm Maxpar Pathsetter, which was a collaborative effort between these two companies.

DISCLOSURES

Fluidigm, Cell-ID, CyTOF, EQ, Helios, Maxpar, and Pathsetter are trademarks and/or registered trademarks of Fluidigm Corporation in the United States and/or other countries. All other trademarks are the sole property of their respective owners. For research use only, not for use in diagnostic procedures.

REFERENCES

Bagwell, C. (2010). Probability state modeling: A new paradigm for cytometric analysis. In V. Litwin & P. Marder (Eds.), *Flow cytometry in drug discovery and development* (p. 281). Hoboken, NJ: John Wiley and Sons Inc.

Bagwell, C. B. (2018). Chapter 2: High-dimensional modeling for cytometry: Building rock solid models using GemStonetm™ and Verity Cen-se'™ high-dimensional t-SNE mapping. In T. S. Hawley & R. G. Hawley (Eds.), *Methods in molecular biology* (Vol. 1678, p. 2018). New York: Springer Science+Business Media LLC.

Bagwell, C. B., Hunsberger, B. C., Herbert, D. J., Munson, M. E., Hill, B. L., Bray, C. M., & Preffer, F. I. (2015). Probability state modeling theory. *Cytometry Part A*, *87*, 646–660.

Bagwell, C. B., Leipold, M., Maecker, H., & Stelzer, G. (2016). *High-dimensional modeling of peripheral blood mononuclear cells from a Helios Instrument*. Seattle, Washington: Washington State Convention Center.

Blazkova, J., Gupta, S., Liu, Y., Gaudilliere, B., Ganio, E. A., Bolen, C. R., ... Furman, D. (2017). Multicenter systems analysis of human blood reveals immature neutrophils in males and during pregnancy. *Journal of Immunology*, *198*, 2479–2488.

Finak, G., Langweiler, M., Jaimes, M., Malek, M., Taghiyar, J., Korin, Y., ... JP, M. C. (2016). Standardizing flow cytometry immunophenotyping analysis from the human ImmunoPhenotyping consortium. *Scientific Reports*, *6*, 20686.

Fluidigm (2018). Maxpar Human Immune Monitoring Panel Kit Cell Staining and Data Acquisition. In: Fluidigm, editor. PN PRD027 C1 Protocol.

Herbert, D., Miller, D., & Bagwell, C. (2012). Automated analysis of flow cytometric data for CD34+ stem cell enumeration using a probability state model. *Cytometry Part B, Clinical Cytometry*, *82B*, 313–318.

Inokuma, M. S., Maino, V. C., & Bagwell, C. B. (2013). Probability state modeling of memory CD8(+) T-cell differentiation. *Journal of Immunological Methods*, *397*, 8–17.

Leipold, M. D., Obermoser, G., Fenwick, C., Kleinstuber, K., Rashidi, N., McNevin, J. P., ... Maecker, H. T. (2018). Comparison of CyTOF assays across sites: Results of a six-center pilot study. *Journal of Immunological Methods*, *453*, 37–43.

Li, S., Majonis, D., Bagwell, C. B., Hunsberger, B. C., Baranov, V. I., & Ornatsky, O. (2018). An efficient human whole blood workflow using CyTOF technology: A lyophilized 30-plex antibody panel coupled with automated data analysis. *Journal of Immunology*, *200*, 120.2.

Li, S., Majonis, D., Bagwell, C. B., Hunsberger, B. C., Baranov, V. I., & Ornatsky, O. (2019). A robust human immunophenotyping workflow using CyTOF technology coupled with Maxpar Pathsetter, an automated data analysis software. *Journal of Immunology*, *202*.

Maecker, H. T., McCoy, J. P., & Nussenblatt, R. (2012). Standardizing immunophenotyping for the human immunology project. *Nature Reviews Immunology*, *12*, 191–200.

Miller, D. T., Hunsberger, B. C., & Bagwell, C. B. (2012). Automated analysis of GPI-deficient leukocyte flow cytometric data using GemStone. *Cytometry Part B, Clinical Cytometry*, *82*, 319–324.

Ornatsky, O. I., Lou, X., Nitz, M., Schafer, S., Sheldrick, W. S., Baranov, V. I., ... Tanner, S. D. (2008). Study of cell antigens and intracellular DNA by identification of element-containing labels and metallointercalators using inductively coupled plasma mass spectrometry. *Analytical Chemistry*, *80*, 2539–2547.

Picozza, M., Battistini, L., & Borsellino, G. (2013). Mononuclear phagocytes and marker modulation: When CD16 disappears, CD38 takes the stage. *Blood*, *122*, 456–457.

Rahman, A. H., Tordesillas, L., & Berin, M. C. (2016). Heparin reduces non-specific eosinophil staining artifacts in mass cytometry experiments. *Cytometry Part A*, *89*, 601–607.

Seder, R. A., & Almed, R. (2003). Similarities and differences in CD4+ and CD8+ effector and memory T cell generation. *Nature Immunology*, *4*, 835–842.

van der Maaten, L. (2009). Learning a Parametric Embedding by Preserving Local Structure. In AISTATS. TiCC. Tilburg, The Netherlands: Tilburg University.

van der Maaten, L. (2014). Accelerating t-SNE using tree-based algorithms. *Journal of Machine Learning Research*, *15*, 1–21.

van der Maaten, L., & Hinton, G. (2008). Visualizing data using t-SNE. *Journal of Machine Learning Research*, *9*, 2579–2605.

Wong, L., Hill, B. L., Hunsberger, B. C., Bagwell, C. B., Curtis, A. D., & Davis, B. H. (2014). Automated analysis of flow cytometric data for measuring neutrophil CD64 expression using a multi-instrument compatible probability state model. *Cytometry Part B, Clinical Cytometry*, *88*(4), 227–235.

Wong, L., Hunsberger, B. C., Bruce Bagwell, C., & Davis, B. H. (2013). Automated quantitation of fetomaternal hemorrhage by flow cytometry for HbF-containing fetal red blood cells using probability state modeling. *International Journal of Laboratory Hematology*, *35*, 548–554.

SUPPORTING INFORMATION

Additional supporting information may be found online in the Supporting Information section at the end of this article.